Estrogen-regulated miRs in bone enhance osteoblast differentiation and matrix mineralization

Michael J. Emch,[1] Zofia Wicik,[2,3] Kirsten G.M. Aspros,[1] Tanja Vukajlovic,[1] Kevin S. Pitel,[1] Anders K. Narum,[4] Megan M. Weivoda,[1,4] Xiaojia Tang,[5] Krishna R. Kalari,[5] Russell T. Turner,[6,7] Urszula T. Iwaniec,[6,7] David G. Monroe,[8] Malayannan Subramaniam,[1] and John R. Hawse[1,9]

[1]Department of Biochemistry and Molecular Biology, Mayo Clinic, Rochester, MN 55905, USA; [2]Department of Neurochemistry, Institute of Psychiatry and Neurology, Sobieskiego 9 Street, 02-957 Warsaw, Poland; [3]Department of Experimental and Clinical Pharmacology, Centre for Preclinical Research and Technology CePT, Medical University of Warsaw, Banacha 1B Street, 02-097 Warsaw, Poland; [4]Hematology, Mayo Clinic, Rochester, MN 55905, USA; [5]Department of Quantitative Health Sciences, Mayo Clinic, Rochester, MN 55905, USA; [6]Skeletal Biology Laboratory, School of Biological and Population Health Sciences, Oregon State University, Corvallis, OR 97331, USA; [7]Center for Healthy Aging Research, Oregon State University, Corvallis, OR 97331, USA; [8]Robert and Arlene Kogod Center on Aging and Division of Endocrinology, Mayo Clinic College of Medicine, Rochester, MN 55905, USA; [9]Department of Cancer Biology, Mayo Clinic, Rochester, MN 55905, USA

Estrogen signaling is critical for the development and maintenance of healthy bone, and age-related decline in estrogen levels contributes to the development of post-menopausal osteoporosis. Most bones consist of a dense cortical shell and an internal mesh-like network of trabecular bone that respond differently to internal and external cues such as hormonal signaling. To date, no study has assessed the transcriptomic differences that occur specifically in cortical and trabecular bone compartments in response to hormonal changes. To investigate this, we employed a mouse model of post-menopausal osteoporosis (ovariectomy, OVX) and estrogen replacement therapy (ERT). mRNA and miR sequencing revealed distinct transcriptomic profiles between cortical and trabecular bone in the setting of OVX and ERT. Seven miRs were identified as likely contributors to the observed estrogen-mediated mRNA expression changes. Of these, four miRs were prioritized for further study and decreased predicted target gene expression in bone cells, enhanced the expression of osteoblast differentiation markers, and altered the mineralization capacity of primary osteoblasts. As such, candidate miRs and miR mimics may have therapeutic relevance for bone loss resulting from estrogen depletion without the unwanted side effects of hormone replacement therapy and therefore represent novel therapeutic approaches to combat diseases of bone loss.

INTRODUCTION

Endocrine signaling, and in particular estrogen signaling, is critical for the maintenance of healthy bone in mammals of both sexes.[1,2] A major consequence of a deficiency in estrogen signaling in adults is the disruption of the balance between bone formation and resorption, with resorption rates outpacing formation rates, leading to net bone loss and ultimately osteoporosis.[3] In the United States, an estimated 43% of adults over 50 have low bone mass, and 10% of adults over 50 have osteoporosis. In the United States, over 2 million osteoporosis-related fractures occur annually at an expected financial burden of $253 billion per year.[4–6] Estrogen replacement therapy (ERT) was once considered the treatment of choice for post-menopausal osteoporosis. However, it has lost this distinction and is now used more sparingly, due in large part to considerable controversy regarding extraskeletal effects of estrogen including cardiovascular disease and breast cancer.[7] Nevertheless, decreased estrogen levels and the subsequent increase in bone resorption following menopause remain a primary driver of osteoporosis.[3] For these reasons, efforts to mimic the agonistic effects of estrogen in bone without the unwanted side effects in other tissues remains of interest and could have a clinically relevant impact in the prevention and treatment of low-bone-mass-related disorders.
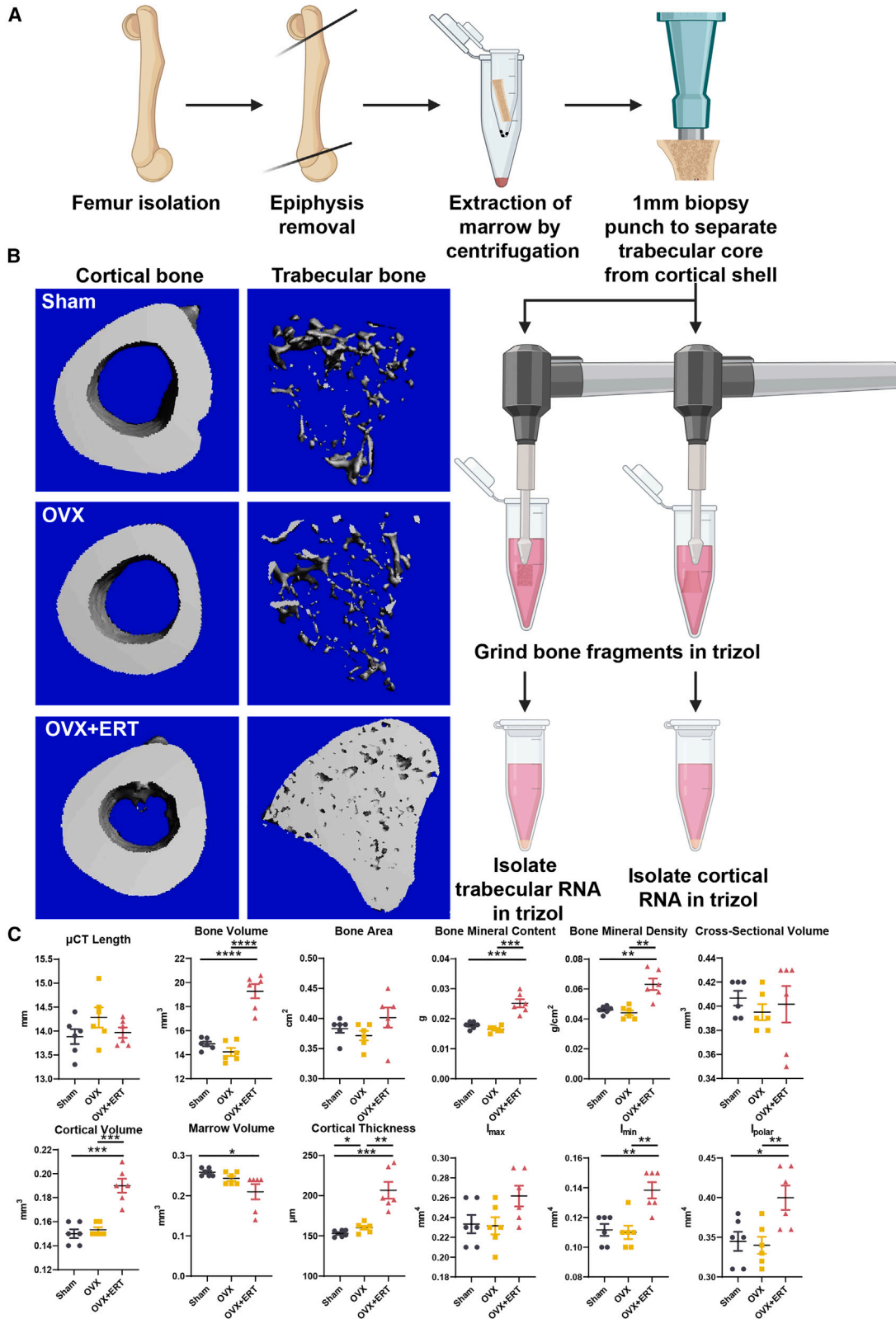
Estrogens exert their effects on cells and tissues primarily through the activation of estrogen receptors (ERs) α and β. ERα and ERβ are nuclear receptor transcription factors that directly bind DNA estrogen response elements to regulate the expression of thousands of genes.[8,9] In addition to regulating the levels of protein coding mRNAs, multiple studies have demonstrated that ERs also regulate numerous nonprotein coding genes such as lncRNAs, miRs, and circRNAs.[10–12] Of these RNA species, the functions and tissue-related consequences of miRNAs are most well-known.[13]

Classically, miRs directly bind multiple mRNAs with complementary sequences to target them for degradation and/or to repress their ability to be translated.[14] Transcription factors are also known to regulate

A. Femur isolation → Epiphysis removal → Extraction of marrow by centrifugation → 1mm biopsy punch to separate trabecular core from cortical shell

B. Cortical bone / Trabecular bone — Sham, OVX, OVX+ERT

Grind bone fragments in trizol

Isolate trabecular RNA in trizol / Isolate cortical RNA in trizol

C. μCT Length, Bone Volume, Bone Area, Bone Mineral Content, Bone Mineral Density, Cross-Sectional Volume, Cortical Volume, Marrow Volume, Cortical Thickness, I_{max}, I_{min}, I_{polar}

(legend on next page)

networks of miRs that can subsequently function in a feedback loop where both miRs and transcription factors regulate a target gene together, with or without additional influence on each other.[14–16] Therefore, miRs have a major influence on the gene expression profiles of a cell given altered expression of their direct mRNA targets as well as downstream impacts influenced by depletion of these direct targets. Regarding estrogen signaling, the contributions of noncoding RNA transcripts in mediating estrogenic responses is poorly characterized, with only two studies having forayed into identifying the ovariectomy-associated miR transcriptome in rodents.[17,18]

For these reasons it was of interest to determine if specific miRs directly targeted by ERs could be identified that mimic the effects of estrogen on bone as an alternative approach toward reducing or slowing the development of age-related osteoporosis. To this end, we utilized an ovariectomy-induced (OVX) mouse model of osteoporosis, with and without ERT, to identify specific miRs that participate in mediating estrogen signaling in bone. RNA sequencing for both mRNAs and miRs was performed on cortical and trabecular bone compartments of the femur. Bioinformatic analyses were used to predict the most relevant miRs responsible for mediating the protein coding gene expression profiles elicited in response to OVX and ERT. The relative expression levels of these miRs were assessed across bone cell types, and their impacts on target gene expression, relevant bone biomarker gene expression, and osteoblast differentiation/mineralization were determined.

RESULTS

Bone/RNA isolation
To ascertain the estrogen-regulated transcriptome in cortical and trabecular bone, mice underwent sham surgery (Sham), ovariectomy plus placebo (OVX), or ovariectomy with estrogen replacement therapy (OVX+ERT). 30 days post surgery and treatment, mice were sacrificed, and the femurs were dissected, and all contaminating muscle and connective tissues were removed. The cortical and trabecular bone compartments were separated from the right femora of each mouse, immersed in trizol, and pulverized, and total RNA was isolated (Figure 1A).

Micro-CT confirmation of surgical and treatment interventions
Prior to proceeding with library preparation and sequencing, the left femur of each mouse was examined via μCT to ensure bone loss and gain in response to OVX and OVX+ERT respectively. As shown in representative 3D reconstruction images, subtle effects of OVX were appreciable with substantial increases in bone mass observed in response to ERT (Figure 1B). More specifically, there were numerical but non-significant decreases in bone volume, bone area, bone mineral content, bone mineral density, cross-sectional volume, marrow volume, and I_{polar} (Figure 1C). Estrogen replacement therapy

resulted in much more dramatic effects with significant increases in bone volume, bone mineral content, bone mineral density, cortical volume, cortical thickness, I_{min}, and I_{polar} (Figure 1C).

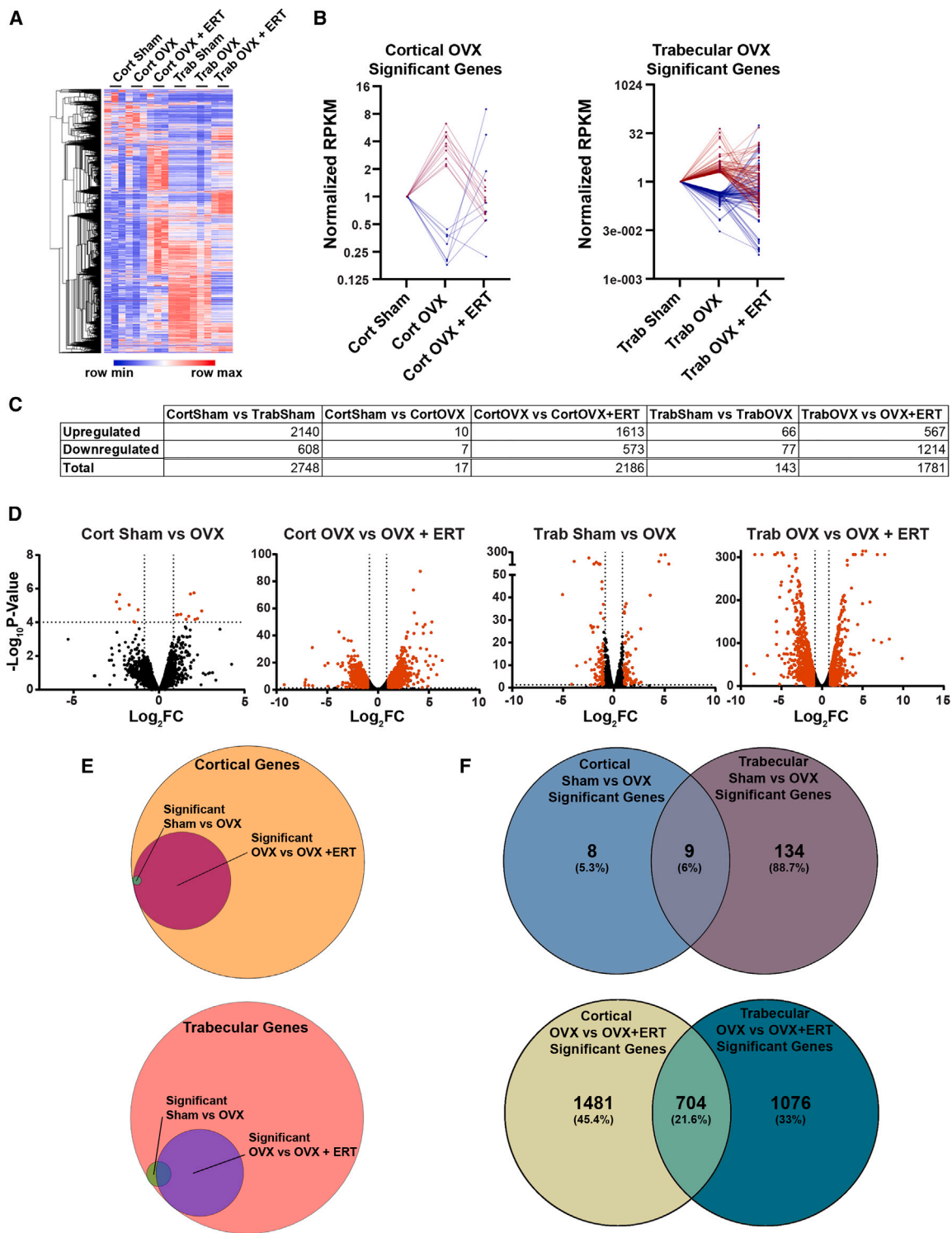### Cortical and trabecular mRNA expression profiling
A total of 12,756 unique transcripts were expressed (reads per kilobase of transcript per million reads mapped [RPKM] > 1) in at least one of the six treatment/bone compartment groups. Of these, 2,748 were differentially expressed (DE) between cortical and trabecular bone (Figures 2A–2C). The effects of OVX on gene expression in cortical bone were minimal, with only 17 DE genes identified (Figures 2C–2E). However, in trabecular bone, the expression of 143 genes were altered in response to OVX (Figures 2C–2E). Only nine of these genes were commonly regulated by OVX in both cortical and trabecular bone (Figure 2F). OVX+ERT led to a much more robust response with 2,186 and 1,781 DE transcripts relative to OVX alone in cortical and trabecular bone compartments, respectively (Figures 2C–2E). Of these, 704 were regulated in both cortical and trabecular bone (Figure 2F). As expected, the majority of mRNAs identified to be altered in expression following OVX were rescued in response to ERT (Figure 2B). A List of all DE genes by comparison can be found in Table S3, a list of gene expression changes by comparison without statistical cutoffs can be found in Table S4, and a list of counts and RPKM for all genes in each replicate can be found in Table S5.

Cortical and trabecular miR expression profiling
In tandem with mRNA sequencing (mRNA-seq), we also performed miR sequencing (miR-seq) using the same RNA samples. Of the 1,915 miRs surveyed we identified 484 miRs meeting our expression criteria in at least 1 sample. Of these 484 miRs, 200 were differentially expressed between sham-operated cortical and trabecular bone compartments (Figures 3A and 3B). As with the mRNA expression profiles, very few DE miRs (13 in total) were identified in cortical bone following OVX (Figure 3B). Similarly, only nine DE miRs were detected in trabecular bone in response to OVX (Figure 3B). Larger numbers of DE miRs were identified in both cortical (47) and trabecular (66) bone following OVX+ERT relative to OVX alone (Figure 3B). There were no miRs commonly regulated in both cortical and trabecular bone in OVX mice, while 11 were regulated in both bone compartments in OVX+ERT animals (Figure 3C). Intriguingly, nearly all DE miRs in both cortical and trabecular bone following OVX were restored to sham levels in OVX+ERT groups, though this restoration is more pronounced in trabecular bone (Figure 3D). As in the mRNA, the most pronounced miR expression changes were in trabecular bone and in response to OVX+ERT (Figure 3E). A list of all DE miRs by comparison can be found in Table S6. A table of all miRs by comparison can be found in Table S7, and the counts for all miRs can be found in Table S8.

Figure 1. RNA extraction from cortical and trabecular bone compartments

(A) Illustration of cortical and trabecular bone isolation procedure followed by tissue homogenization and total RNA extraction (created with biorender.com). (B) Representative μCT images of femoral cortical and trabecular bone compartments 30 days following OVX and ERT. (C) Quantification of multiple bone parameters obtained from each mouse randomized to indicated treatment groups. *p ≤ 0.05, **p ≤ 0.01, and ***p ≤ 0.001 between indicated mouse groups.

Figure 2. mRNA expression profiles in cortical and trabecular bone compartments following OVX and OVX+ERT

(A) Heatmap depicting the relative expression levels of the 12,756 expressed transcripts in cortical and/or trabecular bone. (B) Expression patterns of mRNA transcripts differentially expressed in cortical and trabecular bone of OVX mice and their respective expression levels in OVX+ERT mice normalized to sham controls (log$_2$ scale). (C)

Bioinformatic integration of mRNA-seq and miR-seq datasets

Given the minimal number of DE genes identified in cortical bone, the overall lack of overlap between cortical and trabecular bone transcriptomic changes, and the fact that trabecular bone exhibits rapid and robust changes in response to altered levels of estrogen in both rodents and humans,[19,20] we chose to focus on the mRNAs and miRs regulated in the trabecular compartment.

Using the trabecular miR signature identified in OVX+ERT relative to OVX alone, we performed target prediction analyses to identify estrogen-regulated miRs that were most likely to contribute to the effects of estrogen on mRNA transcripts that were also impacted by ERT. These analyses identified seven miRs (miR-9-5p, miR-129-5p, miR-34a-5p, miR-148a-5p, miR-712-5p, miR-101a-3p, and miR-224-5p) as most likely to contribute to the differential expression changes observed in both bone marker genes and estrogen-regulated genes in these studies. The ERT-mediated expression changes of these miRs, the number of DE mRNAs predicted to be regulated by a given miR that were also found to be downregulated by ERT, and the number of those mRNAs that are involved in bone metabolism or estrogen response are shown in Figure 4A. Given these data, we chose to deprioritize miRs 129-5p and 712-5p due to very low levels of expression. Additionally, miR-34a-5p was excluded due to extensive prior study related to its effects on bone.[21–23] The effects of both OVX and ERT on the four remaining miRs are shown in Figure 4B relative to sham-operated controls.

miR expression across bone cell types and response to estrogen treatment

Next, we profiled the basal expression of each miR in MC3T3 osteoblasts, preosteoclasts, differentiated osteoclasts, and OCY454 osteocytes (Figure 4C). Interestingly, each miR exhibited different expression patterns across these cell lines. All miRs, except for miR-9-5p, were moderately to highly expressed in osteoblasts (Figure 4C). All four miRs were detected in preosteoclasts cells with miRs 101a-3p, 224-3p, and 148a-5p robustly suppressed in differentiated osteoclasts (Figure 4C). Osteocytes exhibited expression of all miRs except miR-148a-5p (Figure 4C). Given the detected increased expression of these four miRs in mouse bone following ERT, it was of interest to determine if these miRs were directly regulated by ERs. Given that primary calvarial osteoblast and MC3T3 cells express relatively low and variable levels of ERα and ERβ, we chose to independently over-express each of these receptors.[24] Briefly, MC3T3-CAR cells were infected with a mouse ERα or ERβ adenovirus, and expression of ERα and ERβ was confirmed via RT-PCR and found to be more highly expressed in their respective cell lines compared with control virus-infected cells (Figure 4D). Control and ERα- and ERβ-expressing MC3T3-CAR cells were treated with ethanol vehicle or 10 nM E2

for 2 and 24 h. miR-101a-3p was immediately induced following E2 treatment in both ERα- and ERβ-expressing cells, an effect that was maintained at 24 h in the ERβ cell line (Figure 4E). miR-148a-5p was strongly induced by E2 following 24 h of treatment in ERα-expressing cells and was not found to be regulated by ERβ (Figure 4E). miR-9-5p was highly expressed in a ligand-independent manner in ERβ-expressing MC3T3-CAR cells, an effect that was attenuated in the presence of E2 (Figure 4E). In ERα-expressing cells, miR-9-5p was upregulated by E2 at both time points (Figure 4E). Of note, miR-224-3p was not expressed in MC3T3-CAR cells, nor was it regulated in a ligand independent or dependent way in ERα- or ERβ-expressing cells (data not shown).

Additionally, we mined publicly available ERα ChIP-seq datasets in various mouse tissues including mammary tissue,[25] uterus, and liver.[26] Strong evidence of ERα binding proximal to miRs 101a, 148a, and 9-2, the parent form of miR-9-5p, was identified in multiple tissues (Figure 4F). There are no publicly available datasets for ERβ ChIP-seq in mouse tissues, making it impossible to determine if ERβ can localize to these chromatin regions as well.

Effects of miR mimics on mRNA expression and osteoblast differentiation and matrix mineralization

We next sought to determine if these four miRs could regulate a random sampling of their predicted mRNA targets in osteoblasts. miR mimics were transfected into primary calvarial osteoblasts, and the resulting effects on target mRNA expression were monitored 72 h later via qPCR. Encouragingly, all three of the randomly selected mRNA targets were significantly downregulated by their respective miR mimics (Figure 5A).

Confident in the mimics' ability to recapitulate ERT-mediated gene expression changes identified by our *in vivo* studies, as well as their ability to be regulated by E2 in bone cells, we next sought to determine their impact on osteoblast differentiation and mineralization. We surmised that if these miRs contribute to the effects of estrogen in bone, miR mimics would partially recapitulate the bone anabolic actions of E2. Using the same primary calvarial osteoblast cells, we next profiled the expression levels of common osteoblast markers at 72 h following miR mimic transfection. We observed upregulation of essential differentiation markers including Runx2, osterix, and osteocalcin, as well as downregulation of the osteoclastogenesis inhibitory factor osteoprotegerin (Opg), by all mimics (Figure 5A). Mixed responses of alkaline phosphatase (Alk Phos), Wnt10b, and Rankl were observed in a miR mimic-dependent manner (Figure 5A).

The common increase in Runx2, osterix, and osteocalcin expression by all mimics suggested that they may be capable of

---

Tabular summary highlighting the number of differentially expressed mRNAs by direction (upregulated vs. downregulated) between treatment groups. (D) Volcano plots of expressed transcripts and their relative fold changes between treatment groups. Significant transcripts (fold change > 2, p ≤ 0.05, FDR ≤ 0.1) are highlighted in orange. (E) Euler plots depicting the overlap of differentially expressed mRNAs in sham vs. OVX and OVX vs. ERT by bone compartment. Size is relative to the total number of expressed transcripts. (F) Venn diagrams indicating the number of unique and commonly regulated mRNA transcripts between the two bone compartments following OVX or OVX+ERT.
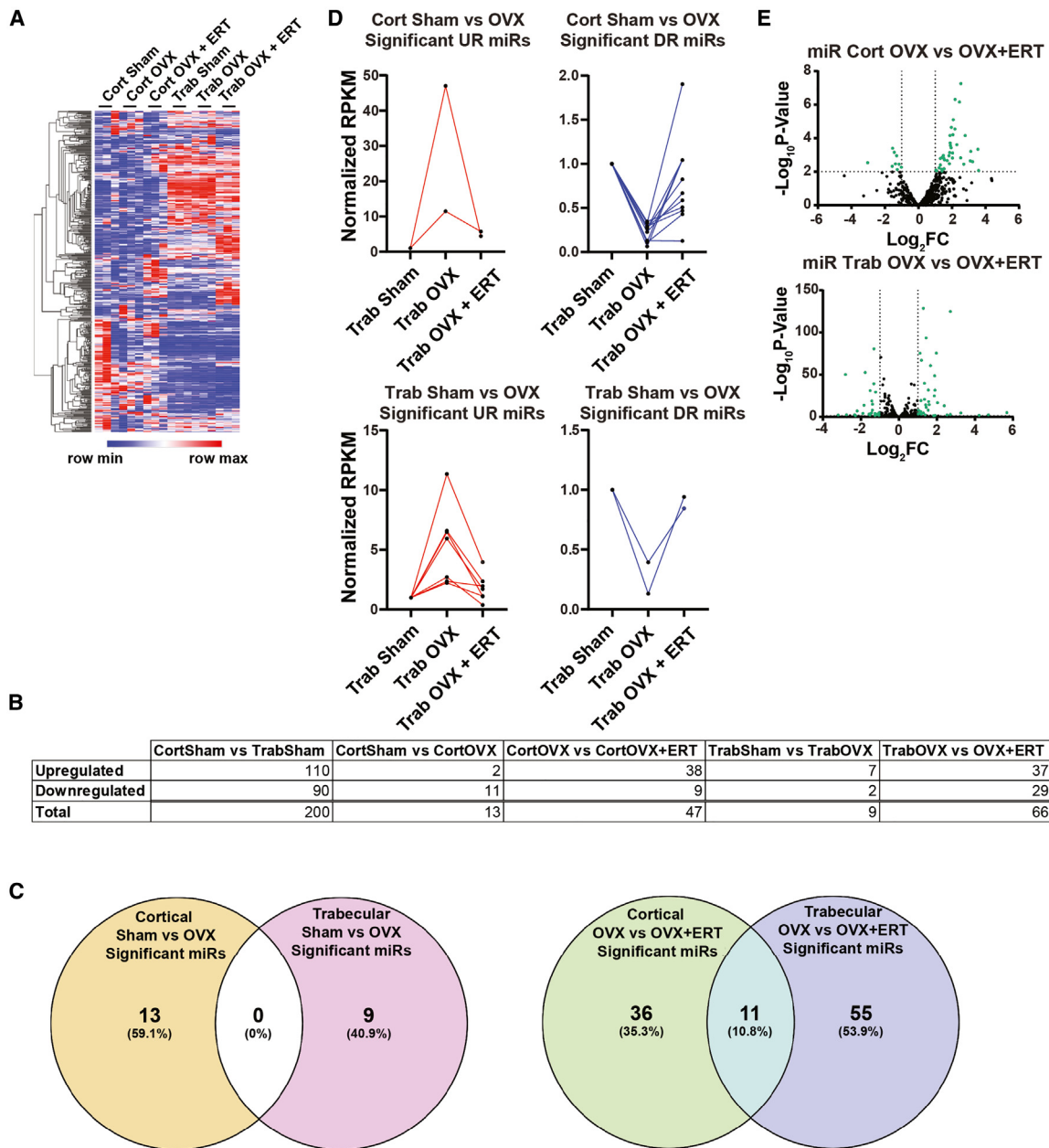
Figure 3. miR expression profiles in cortical and trabecular bone compartments following OVX and OVX+ERT

(A) Heatmap depicting the relative expression levels of the 484 miRs expressed in cortical and/or trabecular bone. (B) Tabular summary highlighting the number of differentially expressed miRs by direction (upregulated vs. downregulated) between the indicated treatment groups. (C) Venn diagrams indicating the number of unique and commonly regulated miRs between the two bone compartments following OVX or OVX+ERT. (D) Expression patterns of miRs identified to be differentially expressed in cortical and trabecular bone of OVX mice and their respective expression levels in OVX+ERT mice, normalized to sham controls. (E) Volcano plots depicting all miRs detected by sequencing and their relative fold changes between indicated treatment groups. miRs exhibiting fold change >2 and FDR ≤ 0.1 are highlighted in green.
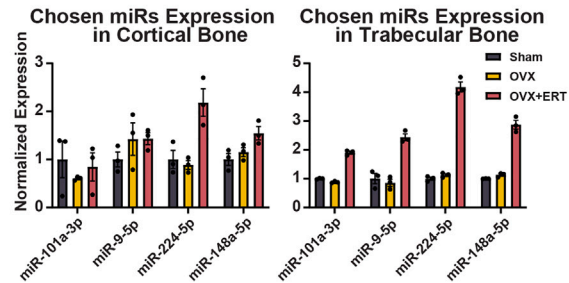
promoting osteoblast differentiation. To test this possibility, we performed a calcein incorporation assay in primary calvarial osteoblast cells using an IncuCyte S3 system. 72 h post miR mimic transfection, calvarial osteoblasts were cultured in differentiation medium for an additional 21 days in the presence of calcein.

Calcein incorporation was significantly enhanced in miR mimic 101a-3p and 148a-5p transfected cells (Figures 5C and 5D). miR mimic 224-5p had no impact on calcein incorporation, while mimic 9-5p robustly decreased calcein incorporation (Figures 5C and 5D).
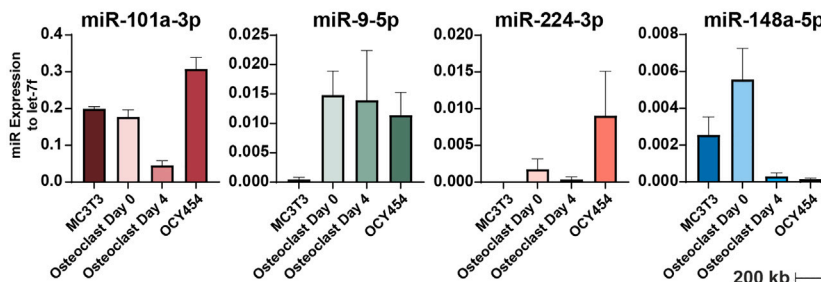
A

	LogFC Trab OVX vs OVX+ERT	miR CPM Trab Sham	miR CPM Trab OVX	miR CPM Trab OVX+ERT	Predicted Total Downstream Gene Count	Predicted Bone Marker Gene Count	Predicted Estrogen Related Gene Count
mmu-miR-9-5p	1.44	38.78	33.14	94.54	276	46	6
mmu-miR-129-5p	1.54	14.81	18.04	55.65	205	35	6
mmu-miR-34a-5p	1.41	53.47	52.63	135.8	190	34	6
mmu-miR-148a-5p	1.34	206.97	234.02	594.23	178	30	4
mmu-miR-712-5p	2.71	2.01	1.13	8.37	137	30	4
mmu-miR-101a-3p	1.11	2196.74	1936.59	4179.48	136	25	6
mmu-miR-224-5p	1.9	49.76	55.98	208.11	119	21	4

B

Chosen miRs Expression in Cortical Bone

Chosen miRs Expression in Trabecular Bone

C

miR-101a-3p

miR-9-5p

miR-224-3p

miR-148a-5p

D

MC3T3 ERα Expression

MC3T3 ERβ Expression

E

MC3T3 miR-101a-3p

MC3T3 miR-9-5p

MC3T3 miR-148a

F

200 kb — mm10 — Mammary / Uterus / Liver / miR-101a

100 kb — mm10 — Mammary / Uterus / Liver / miR-9-2

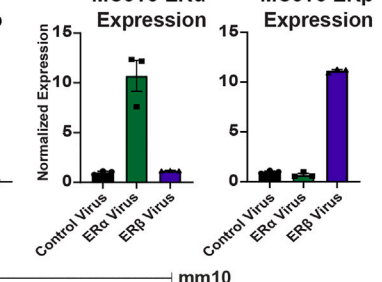200 kb — mm10 — Mammary / Uterus / Liver / miR-224

200 kb — mm10 — Mammary / Uterus / Liver / miR-148a
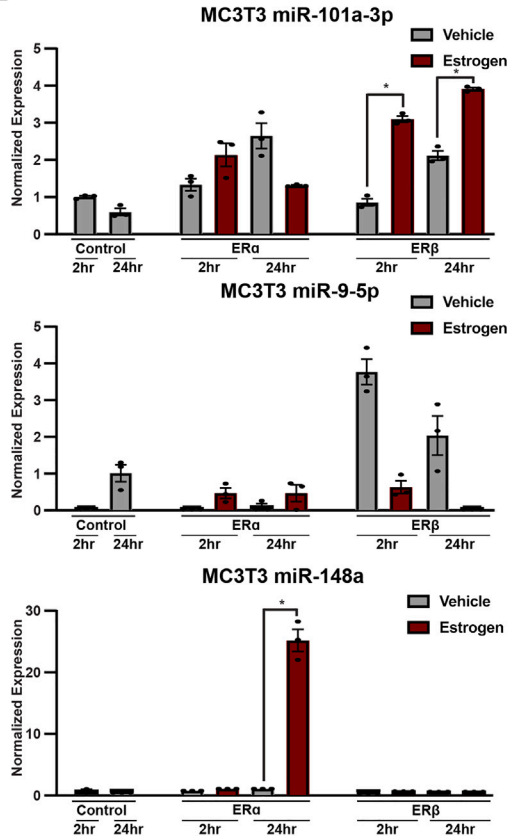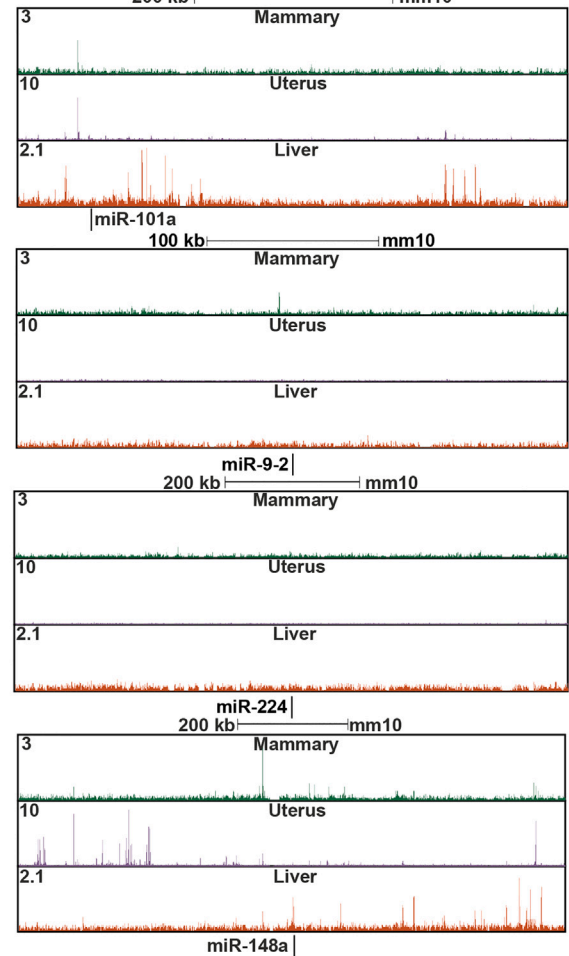
(legend on next page)

DISCUSSION

It is well known that estrogen is protective against bone loss in both men and women and that ERT is an effective treatment strategy that slows the progression of osteopenia and prevents the development of osteoporosis.[2] Here, we sought to determine the type and degree of transcriptomic changes in a murine model of post-menopausal osteoporosis and, from this, to identify miRs that regulate critical downstream effects of estrogen signaling, and as such may ultimately recapitulate the bone-beneficial effects of estrogen on their own. A number of novel observations and data were derived from these studies. Foremost, this is the first reported study to examine the effects of OVX and ERT on both the mRNA and miR transcriptomes in cortical and trabecular bone independently. Second, profound differences in both mRNA and miR expression were observed between cortical and trabecular bone compartments, suggesting non-redundant mechanisms of estrogen signaling in a tissue subtype-specific manner. Third, trabecular bone was impacted greatly by both OVX and ERT compared with the far more stable and overall non-responsive cortical compartment during the 30-day treatment period. Finally, these studies have uncovered a number of miRs that are direct targets of the ERs that were also shown to regulate the expression of multiple ERT-regulated mRNAs in bone, to enhance the expression of critical osteoblasts differentiation genes, and to increase osteoblast mineralization.

Transcription factors, such as the ERs, directly influence gene expression through their interaction with enhancer and promoter elements. However, gene signatures of ER activity are also reflective of the many indirect effects of estrogen that occur due to secondary and tertiary responses controlled by both coding and noncoding RNAs that represent the direct ER targets. The identification and therapeutic utilization of these secondary and tertiary factors hold many advantages over their upstream counterparts including enhanced specificity to tissues of interest, a smaller window of "on target" effects, and corresponding decreases in the likelihood of deleterious side effects. Therapeutic advances on this front have the potential to impact pathways and genes considered hard to target by current approaches. At present, a search of the ClinicalTrials.gov database identifies 1,188 studies that incorporate miRs as biomarkers or therapeutics as part of the trial. Over 150 trials are listed with "oligonucleotide" as a therapeutic intervention, of which nearly 100 are utilizing miRs as a drug. However, none of these focus on osteoporosis.[27] Given the substantial advances that have been made regarding the development of RNA-based therapies,[28] there is a wealth of opportunity to expand the clinical toolkit for the management of bone-related disorders, including osteopenia and osteoporosis.

To this end, we focused on identifying the transcriptomic changes that occur following both OVX and ERT to identify candidate miRs likely to be directly regulated by estrogen and involved in mediating downstream estrogen signaling. A novel consequence of this work relates to the specific analysis of mRNA and miR expression changes in two independent bone compartments (cortical vs. trabecular) and not in whole bone tissue that can also be contaminated by many cell types in the marrow. Not surprisingly, we demonstrate that the basal gene expression profiles between cortical and trabecular bone are largely different, likely due to differences in the abundance of specific bone cell types and/or a reflection of differential activity of specific signaling pathways. Consistent with the fact that trabecular bone reacts to external factors more rapidly than cortical bone and the known increased incidence of osteoporosis in skeletal regions with higher trabecular bone content,[19] many more DE mRNA and miRs were identified in the trabecular compartment of the mouse femur following both OVX and ERT. Bone loss is also more rapid in trabecular bone compared with cortical bone during aging and following menopause[20] and as such represents a target for therapeutics designed to treat low-bone-mass diseases, including the use of miRs or miR mimics.

The present investigation also expands upon a previous study that analyzed miR expression changes in mouse bone following OVX.[29] In their microarray-based design, they also utilized long bones as the source of RNA but combined both the femur and the tibia without prior separation of cortical and trabecular compartments. Their work identified a significantly larger number of DE mRNA following OVX (658) compared with the combined 142 reported here for cortical and trabecular datasets. Interestingly, a total of nine DE miRs were identified in their study in response to OVX, none of which overlapped with the 22 reported here in the cortical or trabecular bone compartments. Further, five of the nine miRs that they identified (miRs 127, 133a, 126, 206, and 378) had significantly lower basal expression in trabecular bone compared with cortical bone in our dataset, with the remaining four exhibiting no differences in expression. However, many factors likely contribute to our discrepant findings including the age and strain of the mice, the aforementioned differences in bone collection, and technical differences between microarray and RNA-seq-based platforms that were employed. Finally, the inclusion of an ERT treatment group in the present study allows for a better

Figure 4. Identification and confirmation of E2-regulated miRs in bone cells

(A) Table of the seven miRs that were differentially expressed in trabecular bone following ERT and identified through ranked target prediction as most likely to contribute to the mRNA expression differences detected in trabecular bone. Each miR's fold change (FC), counts per million sequencing reads (CPM), and the number of mRNAs that they were predicted to target among all differentially expressed mRNAs are reported. (B) Graphical representation of the miR expression patterns in cortical and trabecular bone, normalized to sham expression from the miR sequencing data. (C) Expression of each miR in MC3T3-E1 cells, preosteoclasts (day 0), differentiated osteoclasts (day 4), and OCY454 osteocyte cells. (D) RT-PCR confirmation of ERα and ERβ in MC3T3 cells following adenoviral-mediated infection relative to a control virus. (E) Expression levels of miR-101a-3p, miR-9-5p, and miR-148a-5p in control, ERα-expressing, or ERβ-expressing MC3T3 cells following 72 h of vehicle or estrogen treatment as detected by RT-PCR. miR 224-3p was undetected in all samples and at all time points. (F) ERα ChIP-seq tracts from publicly available mouse mammary, uterus, and liver tissue for the genomic regions encoding each miR. Mean and SEM are indicated for bar graphs; ns, non-significant change; *p $\leq$ 0.05, **p $\leq$ 0.01, and ***p $\leq$ 0.001.

A

B

C

Calcein Incorporation

D
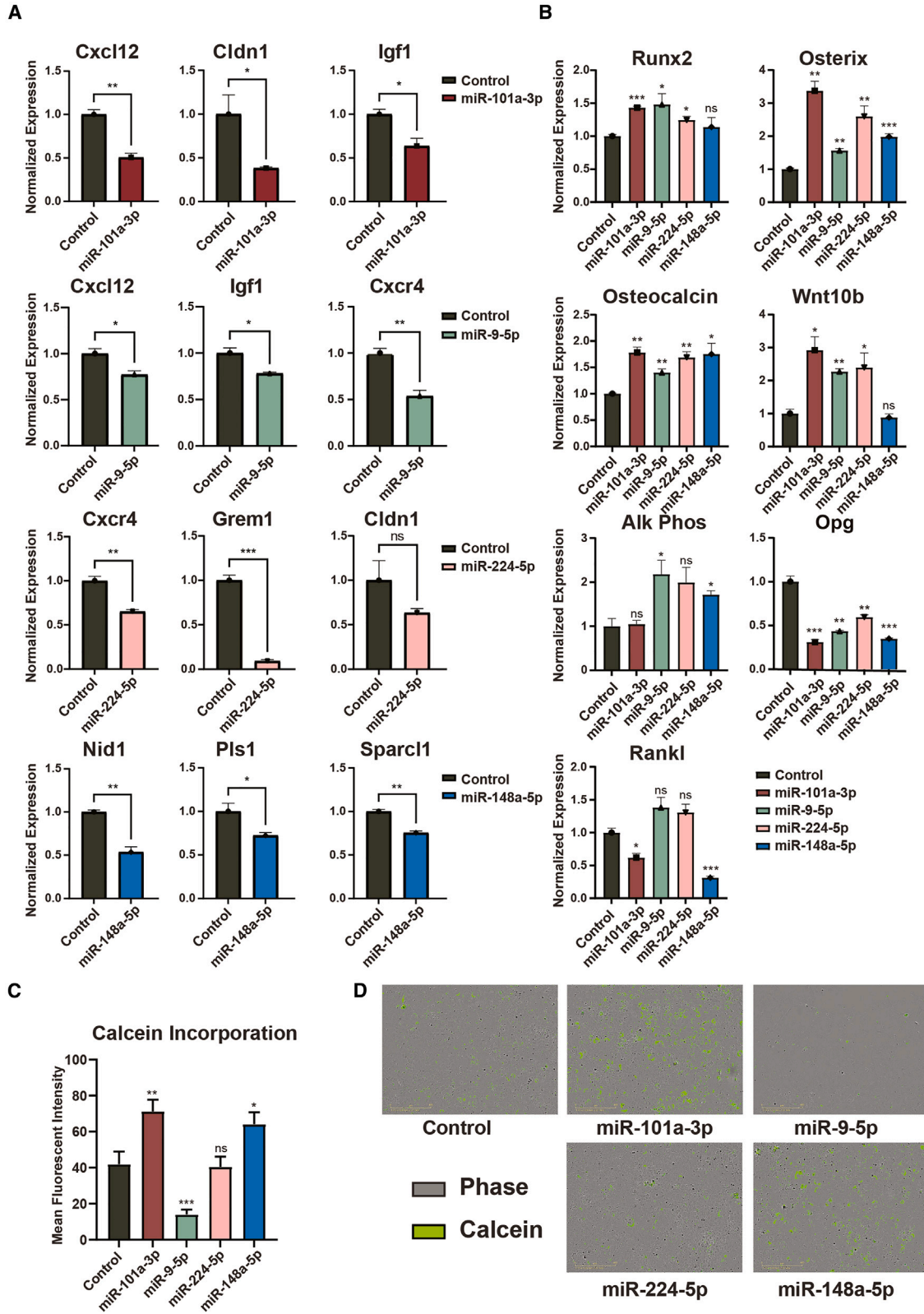
(legend on next page)

assessment of miRs and mRNAs likely to be directly regulated by estrogen and not due to other systemic effects of OVX alone.

Impressively, our bioinformatic analyses were able to identify seven high-confidence miRs that were estrogen regulated and involved in both estrogen signaling and bone metabolism. Additionally, the accuracy of this approach in linking these identified miRs with predicted mRNA targets that were also differentially expressed *in vivo* following ERT was impressive, especially given that our prediction was based on *in vivo* data and our confirmation on *in vitro* observation. The four miRs chosen for further study are relatively unknown with regard to bone and estrogen research. Interestingly, these miRs were expressed across multiple bone cell types, suggesting that they have the potential to dynamically modulate estrogen responses in the skeleton. miR-101a-3p has been shown to enhance IL1β-induced chondrocyte apoptosis.[30] The addition of an exo-miR-9-5p mimetic in rats was shown to significantly improve the rate of cartilage healing in a rheumatoid arthritis model system.[31] Additionally, established links between miR-9-5p and ERα have been described, with miR-9-5p decreasing the expression of ERα in a model of hepatocellular carcinoma.[32,33] To our knowledge, no known links between miR-148a-5p or miR-224-3p in the fields of bone or estrogen research have been reported.

Given the lack of information regarding the potential functions of these miRs in bone cells or the skeleton, we sought to further investigate their biological implications in primary and immortalized calvarial osteoblasts. miRs 101a-3p, 148a-5p, and 9-5p were found to be immediately upregulated by ERα, ERβ, or both in response to short-term E2 treatment, while miR-224-5p was not detected in MC3T3 cells under any treatment condition. In agreement with these findings, ChIP-seq based ER binding sites near the genomic loci for miR 101a-3p, 148a-5p, and 9-5p were identified in one or more estrogen-responsive target tissues of mice with no peaks found in proximity to miR-224-5p. Combined, these discoveries lend confidence that at least three of these four miRs are direct ER targets and therefore are likely to contribute to the effects of E2 in bone. Indeed, mimics of all four miRs enhanced the expression of Runx2, osterix, and osteocalcin, factors essential for the differentiation and function of osteoblasts,[34] the primary cell type responsible for synthesizing bone tissue.[35] Impressively, mimics of miRs 101a-3p and 148a-5p increased osteoblast mineralization as measured by calcein incorporation despite the fact that these mimics were only transfected into primary calvarial osteoblasts once, which occurred over 3 weeks prior to completion of the differentiation and mineralization assays. A common feature of miR mimics 101a-3p and 148a-5p that was not observed by 9-5p or 224-5p was the suppression of Rankl expression,

a factor critical for the differentiation and function of bone resorbing osteoclasts *in vivo*,[36] suggesting that they may elicit bone anabolic effects in the absence of increased rates of bone turnover. These findings suggest that therapeutic strategies employing such miR mimics may not require frequent administration in order to achieve clinically meaningful responses, a possibility that must be explored in future mouse and rat models of post-menopausal osteoporosis.

In summary, using a pre-menopausal mouse model of osteoporosis and high-throughput mRNA and miR sequencing, we have defined the transcriptomic changes that occur in cortical and trabecular bone following OVX and ERT. Bioinformatic analyses identified seven specific miRs that exhibited altered expression in response to OVX and ERT as most likely to contribute to changes in mRNA expression in the same bone compartments. Of these, four were chosen for further study based on their overall expression levels and lack of data linking them to estrogen signaling or bone disease. miRs 101a-3p, 148a-5p, and 9-5p were shown to be estrogen regulated, capable of decreasing the expression of their predicted target genes in bone cells, and able to enhance the expression of critical osteoblast differentiation factors in primary calvarial osteoblasts. Further, miR mimics of 101a-3p and 148a-5p increased the rates of bone matrix mineralization *in vitro*.

There are several limitations to our study including the age of animals utilized in this report. We chose to perform surgical procedures at a young age to prevent the occurrence of any endogenous estrogenic effects from occurring. However, the miRs identified were confirmed to be estrogen regulated, and future studies aimed at assessing their *in vivo* effects on bone should be studied across age groups. Additionally, it is difficult to extrapolate the bulk RNA-seq studied as a function of specific cell types within bone. Our *in vitro* studies confirmed that these miRs are detectable in osteoblasts, osteoclasts, and osteocytes, but further work is required to elucidate their molecular mechanisms of action within a given cell. Another limitation of this study potentially relates to the dose of estradiol used for the *in vivo* studies. As reflected in the micro-CT images, the bone mass following estradiol supplementation exceeds that observed in sham-operated animals and thus can be considered supra-physiological. However, this dose has been used in many previous studies[37,38] and was chosen to maximize the number and magnitude of mRNA and miR expression changes detected in the RNA-seq studies. Finally, there are no relevant human datasets that include cortical vs. trabecular bone biopsies from pre- and post-menopausal women, as well as women receiving ERT, to validate our findings. Nevertheless, our studies have identified multiple miRs that are likely to mediate the bone-beneficial effects of estrogen on the skeleton and therefore warrant further *in vivo*

Figure 5. Impact of miR mimics on predicted target mRNA levels, expression of essential osteoblast differentiation genes, and mineralization of matrix formed by primary calvarial osteoblasts

(A) Effects of miR mimics on three predicted, and randomly selected, target genes in primary calvarial osteoblasts 72 h post transfection as determined by RT-PCR. (B) Expression levels of important osteoblast marker genes in primary calvarial osteoblasts 72 h post transfection with miR mimics as determined by RT-PCR. (C) Primary calvarial osteoblast differentiation assay as determined by IncuCyte assessment of calcein incorporation 21 days post transfection of miR mimics. (D) Representative images of fluorescent calcein incorporation. Mean and SEM; ns, non-significant change; *p ≤ 0.05, **p ≤ 0.01, and ***p ≤ 0.001.

study to determine their ability to prevent bone loss in post-menopausal models of osteoporosis. If successful, such discoveries would pave the way for a new class of oligonucleotide-based drugs to slow bone loss and prevent osteoporosis in humans without the unwanted side effects of hormonal therapies.

MATERIAL AND METHODS

Animals
A total of 18 (six per group) 8-week-old female C57BL/6 mice were randomized to sham+placebo, OVX+placebo, or OVX+ERT treatment groups. Sham and OVX surgeries were performed as previously described.[39] Immediately following surgery, a 1.88 μg 17β-estradiol 30-day slow-release pellet, or placebo pellet, (Innovative Research of America, Sarasota, FL) was implanted subcutaneously in the nape of the neck between the shoulder blades. 30 days post-surgery, mice were sacrificed, and the femurs were collected for μCT imaging and cortical/trabecular bone separation. All mice were housed in a temperature-controlled room ($22°C \pm 2°C$) with a standard light and dark cycle of 12 h with unrestricted access to water and standard laboratory chow. The protocol was approved by the Mayo Clinic Institutional Animal Care and Use Committee (Permit Number: A5735).

μCT imaging
μCT imaging was performed as previously described.[39,40] Briefly the femora were placed in a Scano μCT40 scanner (Scano, Basserdorf, Switzerland) and scanned with the following settings: a voxel size of 12 μm × 12 μm x 12 μm, 55 kVp X-ray voltage, 145 μA intensity, 200 ms integration time, bone segmentation 245, and filtering parameters sigma 0.8 and support 1. Cortical bone was assessed in the mid femur diaphysis and trabecular bone evaluated in the distal femur metaphysis. 3D reconstruction images were generated to confirm bone loss and gain in response to OVX and ERT respectively.

Isolation of cortical and trabecular bone compartments
Manual separation of cortical and trabecular bone was adapted from Kelly et al.[41] Briefly, all muscle and connective tissue was removed from the femurs using tweezers and sterilized Kimwipes. Both epiphyses were cut and removed, and the marrow was cleared by centrifugation. Trabecular bone was isolated from each end of the femoral shaft using a 1-mm biopsy punch and immediately placed into TRIzol (Invitrogen, Waltham, MA). The remaining cortical shell was trimmed on each end, and the remaining mid diaphysis consisting of cortical bone was placed in a separate microcentrifuge tube of TRIzol. Bone tissues were homogenized using an ULTRA-TURRAX homogenizer (IKA Works, Wilmington, NC), and total RNA, including miRs, was extracted using the Qiagen miRNeasy kit (Qiagen, Hilden, GER). Resulting RNA was further purified on a Qiagen RNeasy Mini spin column.

mRNA and miR sequencing
Prior to sequencing, equal amounts of cortical or trabecular RNA from two individual mice were pooled to generate three replicate samples for each bone compartment and treatment group. Library preparation and mRNA sequencing were performed by the Mayo Clinic Genome Analysis core, and secondary analysis was performed by the Mayo Clinic Bioinformatics core using the Map-Rseq pipeline.[42] To remove lowly expressed genes, an RPKM >1 in at least one sample was used as a cutoff. miR sequencing was performed using CAP-miRSeq v1.1.[43] A count threshold ≥ 5 was used to remove lowly expressed miRs. Differential expression of mRNA and miR data was calculated by exact tests using edgeR.[44] Statistical cutoffs used to identify DE mRNAs and miRs were a fold change >2, a p value ≤ 0.05, and a false discovery rate ≤ 0.1. Venn diagrams were generated using Venny (BioinfoGP, Spanish National Biotechnology Center, Madrid, ES) to determine overlap between treatment groups and bone compartments.

Predicted mRNA targets of DE miRs
In order to identify mRNA targets of DE miRNAs, we first grouped expression datasets into pairs including DE miRNAs and DE mRNA. Target predictions were performed using the multimiR package,[45] with a prediction score cutoff of 30%, only in the trabecular datasets given the small number of transcripts identified in cortical samples. Two independent predictions, (1) upregulated DE miRs vs. downregulated DE mRNAs and (2) downregulated DE miRs vs. upregulated DE mRNAs, were performed.

Gene lists
Human genes associated with the estrogen-related signaling pathways were obtained from the following databases: KEGG (estrogen signaling pathway), PharmGKB (estrogen metabolism pathway), SMPDB (androgen and estrogen metabolism), Wikipathways (estrogen receptor pathway), Wikipathways (ESR-mediated signaling), Wikipathways (estrogen metabolism), Wikipathways (estrogen signaling pathway), HumanCyc (estradiol biosynthesis II), PID (validated nuclear estrogen receptor alpha network), PID (plasma membrane estrogen receptor signaling), BioCarta (carm1 and regulation of the estrogen receptor), Reactome (estrogen biosynthesis), BioCarta (estrogen responsive protein Efp controls cell cycle and breast tumor growth), PID (validated nuclear estrogen receptor beta network), HumanCyc (estradiol biosynthesis I), BioCarta (pelp1 modulation of estrogen receptor activity), Reactome (estrogen-dependent gene expression), EHMN (androgen and estrogen biosynthesis and metabolism), Reactome (RUNX1 regulates estrogen receptor-mediated transcription), and Reactome (ESR-mediated signaling). Human genes associated with bone metabolism were obtained from Table S1 of a related publication.[46] We excluded the "Genetics.in.Arterial.Calcification" gene list given that this dataset is confounded by other diseases contributing to arterial calcification such as diabetes mellitus, dyslipidemia, hypertension, gender, renal health, and inflammation. Different gene lists were combined with each other using NCBI_synonyms() and lists_combiner() R functions from the wizbionet R package.[47]

Translation of human gene symbols into mouse orthologs
Translation of the human estrogen gene lists and bone metabolism-related gene lists into mouse orthologs was performed using the

Ensembl Biomart database.[48,49] For further analysis, we used only genes that were present on any of the estrogen-related or bone metabolism-related gene lists and that had orthologs with high (equal to 1) mouse orthology confidence scores. These gene lists with their predicted orthologs are included in Table S1.

Data aggregation and ranking

Data aggregation and prioritization were performed using functions col_aggrecounter() and clusterizer_oneR() from the R package wizbionet to prioritize miRs most likely to contribute to the identified gene expression changes. These were miRs that were predicted to target DE genes within the first two clusters of all three analyzed gene lists (any DE genes with opposite regulation between OVX and OVX+ERT, estrogen-related DE genes, and bone metabolism-related DE genes).

Cell lines

Primary calvarial osteoblast cultures were derived from 3-day-old C57BL/6 mice as previously described.[50,51] Briefly, the calvarium was removed, washed with PBS, and minced in Hanks balanced saline solution (Sigma-Aldrich, St. Louis, MO) containing 4 mg/ml BSA and 4 mg/ml collagenase 2 for several hours at 37°C. The dissociated cells were centrifuged at 221 x g for 5 min and resuspended and maintained in α-MEM (Invitrogen, Carlsbad, CA) with 10% FBS (Gibco Waltham, MA, Gemini Bio, Sacramento, CA). The cells are maintained in α-MEM (Invitrogen, Carlsbad, CA) with 10% FBS (Gemini Bio-Products, West Sacramento, CA) and 1% Anti-Anti antibiotic-antimycotic (Gibco Waltham, MA). Cultures were passaged no more than four times, and low-passage cultures were used for all experiments.

The osteoclast precursors were derived and differentiated as previously described.[52] Skeletally mature (4 months of age) female C57BL/6 mice were euthanized, and long bones were isolated to obtain mouse bone marrow. Bone marrow was flushed with sterile PBS, and red blood cells were lysed with Red Cell Lysis Buffer (eBioscience, San Diego, CA). Whole bone marrow cells were cultured overnight with 30 ng/mL recombinant murine M-CSF (R&D Systems, Minneapolis, MN). Non-adherent cells were collected and plated at a density of 4 x 10^5 cells/well in 24-well plates in osteoclast differentiation medium (alpha-MEM, 10% FBS, 1x antibiotic/antimycotic, 20 ng/mL rmM-CSF, 50 ng/mL recombinant murine RANKL). Alternatively, the remaining progenitors were collected for osteoclast progenitor RNA isolation. Osteoclast culture media was replaced on differentiation cells after 72 h. RNA was collected from differentiated osteoclasts 24 h later (4 days of differentiation total).

The OCY454 osteocyte cell line was provided by Dr. Pajevic's laboratory and cultured as previously described.[53] MC3T3-E1 cells were obtained from ATCC and maintained in alpha-MEM containing 10% FBS and 1% AA. The derivative MC3T3-E1-CAR cells were developed by stably integrating the coxsackievirus and adenovirus receptor.

miR mimics

miRIDIAN miR mimics were purchased from Dharmacon (Lafayette, CO) and transfected into calvarial osteoblast cell lines using DharmaFECT #1 following the recommended protocol at a final concentration of 25 nM. 72 h post transfection, medium was replaced with osteoblast differentiation medium (α-MEM + 10% FBS + 50 μg/ml ascorbic acid + 4 mM β-glycerol phosphate). Following 4 days of differentiation, total RNA was isolated as described above. To examine gene expression, cDNA was generated using the iScript cDNA Synthesis Kit (Bio-Rad, Hercules, CA), and qRT-PCR was performed as previously described[54] to determine changes in candidate gene expression compared with housekeeping controls. qRT-PCR was performed using PerfectCT SYBR Green Fast Mix (Quanta Biosciences, Gaithersburg, MD) in a Bio-Rad CFX Real-Time PCR detection system (Bio-Rad, Hercules, CA), and data were analyzed using the $2^{-\Delta\Delta Ct}$ method. Primer sequences are included in Table S2. Statistical significance was determined using the Student's t test and performed using GraphPad Prism version 9.3.1 (GraphPad Software, San Diego, CA).

Effects of estrogen signaling on miR expression

Mouse ERα and ERβ adenoviruses (Vector Biolabs, Malvern, PA) were utilized to confer expression of these two receptors in MC3T3-E1-CAR cells following standard techniques with 10 μg/mL Polybrene (Sigma-Aldrich). 2 days post infection, cells were treated with ethanol vehicle or 10 nM estradiol for 2 and 24 h. Total RNA was isolated as described above, and miR expression was assayed using the Taqman Advanced miRNA assay kit (Applied Biosystems, Waltham, MA, USA) following the manufacturer's instructions. miR-let-7f-5p was used to normalize expression[55] using the $2^{-\Delta\Delta Ct}$ method.

Effects of miR mimics on osteoblast differentiation

Calvarial osteoblast differentiation was assessed using calcein incorporation and an IncuCyte S3 system (Sartorius, Goettingen, Germany) as described previously.[56] Briefly, cells were plated in 12-well plates and transfected with miR mimics as described above. 3 days following transfection, differentiation medium containing 1 μM calcein (Sigma-Aldrich, St. Louis, MO) was added and refreshed every 3–4 days. Following 21 days of differentiation, calcein was removed, and cells were washed 2 times with PBS. Differentiation medium without calcein was added, and the cells were imaged in the IncuCyte S3 system with the green and phase channels. Calcein incorporation (green fluorescence) was quantified using the Incucyte software package. Green signal was defined using an adaptive segmentation with a threshold adjustment (GCU 0.25). Additionally, a minimum area filter of 1500 μm^2 and a minimum mean intensity filter of 8.0 were applied. Data are representative of 16 replicate images.

DATA AVAILABILITY

mRNA-seq and miR-seq raw data have been deposited in GEO with the following accession numbers respectively: GSE222752 and GSE221729.

SUPPLEMENTAL INFORMATION

ACKNOWLEDGMENTS

AUTHOR CONTRIBUTIONS

M.J.E., K.G.MA., D.G.M., M.S., and J.R.H. developed the study concept and design; M.J.E., K.G.MA., T.V., K.S.P., A.K.N., M.M.W., R.T.T., U.T.I., M.S., and J.R.H. collected and assembled the data; M.J.E., Z.W., X.T., K.R.K., R.T.T., U.T.I., D.G.M., M.S., and J.R.H. performed data analysis and interpretation; M.J.E. and J.R.H. wrote the manuscript; and all authors read, reviewed, and approved the final version of the manuscript.

DECLARATION OF INTERESTS

The authors declare no conflicts of interest.

REFERENCES

1. Agas, D., Lacava, G., and Sabbieti, M.G. (2018). Bone and bone marrow disruption by endocrine-active substances. J. Cell. Physiol. *234*, 192–213.

2. Khosla, S., and Monroe, D.G. (2018). Regulation of bone metabolism by sex steroids. Cold Spring Harb. Perspect. Med. *8*, a031211.

3. Khosla, S., Oursler, M.J., and Monroe, D.G. (2012). Estrogen and the skeleton. Trends Endocrinol. Metabol. *23*, 576–581.

4. Arceo-Mendoza, R.M., and Camacho, P.M. (2021). Postmenopausal osteoporosis: latest guidelines. Endocrinol Metab. Clin. N. Am. *50*, 167–178.

5. Burge, R., Dawson-Hughes, B., Solomon, D.H., Wong, J.B., King, A., and Tosteson, A. (2007). Incidence and economic burden of osteoporosis-related fractures in the United States, 2005-2025. J. Bone Miner. Res. *22*, 465–475.

6. Wright, N.C., Looker, A.C., Saag, K.G., Curtis, J.R., Delzell, E.S., Randall, S., and Dawson-Hughes, B. (2014). The recent prevalence of osteoporosis and low bone mass in the United States based on bone mineral density at the femoral neck or lumbar spine. J. Bone Miner. Res. *29*, 2520–2526.

7. Camacho, P.M., Petak, S.M., Binkley, N., Diab, D.L., Eldeiry, L.S., Farooki, A., Harris, S.T., Hurley, D.L., Kelly, J., Lewiecki, E.M., et al. (2020). American association of clinical endocrinologists/American college of endocrinology clinical practice guidelines for the diagnosis and treatment of postmenopausal osteoporosis-2020 update. Endocr. Pract. *26*, 1–46.

8. Fuentes, N., and Silveyra, P. (2019). Estrogen receptor signaling mechanisms. Adv. Protein Chem. Struct. Biol. *116*, 135–170.

9. Eyster, K.M. (2016). The estrogen receptors: an overview from different perspectives. Methods Mol. Biol. *1366*, 1–10.

10. Cicatiello, L., Mutarelli, M., Grober, O.M.V., Paris, O., Ferraro, L., Ravo, M., Tarallo, R., Luo, S., Schroth, G.P., Seifert, M., et al. (2010). Estrogen receptor alpha controls a gene network in luminal-like breast cancer cells comprising multiple transcription factors and microRNAs. Am. J. Pathol. *176*, 2113–2130.

11. Wang, L., Yi, J., Lu, L.Y., Zhang, Y.Y., Wang, L., Hu, G.S., Liu, Y.C., Ding, J.C., Shen, H.F., Zhao, F.Q., et al. (2021). Estrogen-induced circRNA, circPGR, functions as a ceRNA to promote estrogen receptor-positive breast cancer cell growth by regulating cell cycle-related genes. Theranostics *11*, 1732–1752.

12. Nassa, G., Tarallo, R., Giurato, G., De Filippo, M.R., Ravo, M., Rizzo, F., Stellato, C., Ambrosino, C., Baumann, M., Lietzèn, N., et al. (2014). Post-transcriptional regulation of human breast cancer cell proteome by unliganded estrogen receptor beta via microRNAs. Mol. Cell. Proteomics *13*, 1076–1090.

13. Panni, S., Lovering, R.C., Porras, P., and Orchard, S. (2020). Non-coding RNA regulatory networks. Biochim. Biophys. Acta. Gene Regul. Mech. *1863*, 194417.

14. Arora, S., Rana, R., Chhabra, A., Jaiswal, A., and Rani, V. (2013). miRNA-transcription factor interactions: a combinatorial regulation of gene expression. Mol. Genet. Genom. *288*, 77–87.

15. Maillot, G., Lacroix-Triki, M., Pierredon, S., Gratadou, L., Schmidt, S., Bénès, V., Roché, H., Dalenc, F., Auboeuf, D., Millevoi, S., and Vagner, S. (2009). Widespread estrogen-dependent repression of micrornas involved in breast tumor cell growth. Cancer Res. *69*, 8332–8340.

16. Sukocheva, O.A., Lukina, E., Friedemann, M., Menschikowski, M., Hagelgans, A., and Aliev, G. (2022). The crucial role of epigenetic regulation in breast cancer anti-estrogen resistance: current findings and future perspectives. Semin. Cancer Biol. *82*, 35–59.

17. Xu, X., Zhang, P., Li, X., Liang, Y., Ouyang, K., Xiong, J., Wang, D., and Duan, L. (2020). MicroRNA expression profiling in an ovariectomized rat model of postmenopausal osteoporosis before and after estrogen treatment. Am. J. Transl. Res. *12*, 4251–4263.

18. An, J.H., Ohn, J.H., Song, J.A., Yang, J.Y., Park, H., Choi, H.J., Kim, S.W., Kim, S.Y., Park, W.Y., and Shin, C.S. (2014). Changes of microRNA profile and microRNA-mRNA regulatory network in bones of ovariectomized mice. J. Bus. Manag. Res. *29*, 644–656.

19. Goodyear, S.R., Gibson, I.R., Skakle, J.M.S., Wells, R.P.K., and Aspden, R.M. (2009). A comparison of cortical and trabecular bone from C57 Black 6 mice using Raman spectroscopy. Bone *44*, 899–907.

20. Ott, S.M. (2018). Cortical or trabecular bone: what's the difference? Am. J. Nephrol. *47*, 373–375.

21. Komori, T. (2016). Glucocorticoid signaling and bone biology. Horm. Metab. Res. *48*, 755–763.

22. Liu, H., Dong, Y., Feng, X., Li, L., Jiao, Y., Bai, S., Feng, Z., Yu, H., Li, X., and Zhao, Y. (2019). miR-34a promotes bone regeneration in irradiated bone defects by enhancing osteoblastic differentiation of mesenchymal stromal cells in rats. Stem Cell Res. Ther. *10*, 180.

23. Sun, D., Chen, Y., Liu, X., Huang, G., Cheng, G., Yu, C., and Fang, J. (2022). miR-34a-5p facilitates osteogenic differentiation of bone marrow mesenchymal stem cells and modulates bone metabolism by targeting HDAC1 and promoting ER-alpha transcription. Connect. Tissue Res. *64*, 126–138.

24. Roforth, M.M., Liu, G., Khosla, S., and Monroe, D.G. (2012). Examination of nuclear receptor expression in osteoblasts reveals Rorbeta as an important regulator of osteogenesis. J. Bone Miner. Res. *27*, 891–901.

25. Miranda, T.B., Voss, T.C., Sung, M.H., Baek, S., John, S., Hawkins, M., Grøntved, L., Schiltz, R.L., and Hager, G.L. (2013). Reprogramming the chromatin landscape: interplay of the estrogen and glucocorticoid receptors at the genomic level. Cancer Res. *73*, 5130–5139.

26. Gertz, J., Savic, D., Varley, K.E., Partridge, E.C., Safi, A., Jain, P., Cooper, G.M., Reddy, T.E., Crawford, G.E., and Myers, R.M. (2013). Distinct properties of cell-type-specific and shared transcription factor binding sites. Mol. Cell. *52*, 25–36.

27. Zogg, H., Singh, R., and Ro, S. (2022). Current advances in RNA therapeutics for human diseases. Int. J. Mol. Sci. *23*, 2736.

28. Chakraborty, C., Sharma, A.R., Sharma, G., and Lee, S.S. (2021). Therapeutic advances of miRNAs: a preclinical and clinical update. J. Adv. Res. *28*, 127–138.

29. An, J.H., Ohn, J.H., Song, J.A., Yang, J.Y., Park, H., Choi, H.J., Kim, S.W., Kim, S.Y., Park, W.Y., and Shin, C.S. (2014). Changes of microRNA profile and microRNA-mRNA regulatory network in bones of ovariectomized mice. J. Bone Miner. Res. *29*, 644–656.

30. Mao, D., Wu, M., Wei, J., Zhou, X., Yang, L., and Chen, F. (2021). MicroRNA-101a-3p could be involved in the pathogenesis of temporomandibular joint osteoarthritis by mediating UBE2D1 and FZD4. J. Oral Pathol. Med. 50, 236–243.

31. Zheng, C., Bai, C., Sun, Q., Zhang, F., Yu, Q., Zhao, X., Kang, S., Li, J., and Jia, Y. (2020). Long noncoding RNA XIST regulates osteogenic differentiation of human bone marrow mesenchymal stem cells by targeting miR-9-5p. Mech. Dev. 162, 103612.

32. Wang, L., Cui, M., Cheng, D., Qu, F., Yu, J., Wei, Y., Cheng, L., Wu, X., and Liu, X. (2021). miR-9-5p facilitates hepatocellular carcinoma cell proliferation, migration and invasion by targeting ESR1. Mol. Cell. Biochem. 476, 575–583.

33. Barbano, R., Pasculli, B., Rendina, M., Fontana, A., Fusilli, C., Copetti, M., Castellana, S., Valori, V.M., Morritti, M., Graziano, P., et al. (2017). Stepwise analysis of MIR9 loci identifies miR-9-5p to be involved in Oestrogen regulated pathways in breast cancer patients. Sci. Rep. 7, 45283.

34. Capulli, M., Paone, R., and Rucci, N. (2014). Osteoblast and osteocyte: games without frontiers. Arch. Biochem. Biophys. 561, 3–12.

35. Ponzetti, M., and Rucci, N. (2021). Osteoblast differentiation and signaling: established concepts and emerging topics. Int. J. Mol. Sci. 22, 6651.

36. Elango, J., Bao, B., and Wu, W. (2021). The hidden secrets of soluble RANKL in bone biology. Cytokine 144, 155559.

37. Subramaniam, M., Pitel, K.S., Bruinsma, E.S., Monroe, D.G., and Hawse, J.R. (2018). TIEG and estrogen modulate SOST expression in the murine skeleton. J. Cell. Physiol. 233, 3540–3551.

38. Subramaniam, M., Hawse, J.R., Bruinsma, E.S., Grygo, S.B., Cicek, M., Oursler, M.J., and Spelsberg, T.C. (2010). TGFbeta inducible early gene-1 directly binds to, and represses, the OPG promoter in osteoblasts. Biochem. Biophys. Res. Commun. 392, 72–76.

39. Mann, S.N., Pitel, K.S., Nelson-Holte, M.H., Iwaniec, U.T., Turner, R.T., Sathiaseelan, R., Kirkland, J.L., Schneider, A., Morris, K.T., Malayannan, S., et al. (2020). 17alpha-Estradiol prevents ovariectomy-mediated obesity and bone loss. Exp. Gerontol. 142, 111113.

40. Lee, B., Iwaniec, U.T., Turner, R.T., Lin, Y.W., Clarke, B.L., Gingery, A., and Wei, L.N. (2017). RIP140 in monocytes/macrophages regulates osteoclast differentiation and bone homeostasis. JCI Insight 2, e90517.

41. Kelly, N.H., Schimenti, J.C., Patrick Ross, F., and van der Meulen, M.C.H. (2014). A method for isolating high quality RNA from mouse cortical and cancellous bone. Bone 68, 1–5.

42. Kalari, K.R., Nair, A.A., Bhavsar, J.D., O'Brien, D.R., Davila, J.I., Bockol, M.A., Nie, J., Tang, X., Baheti, S., Doughty, J.B., et al. (2014). MAP-RSeq: Mayo analysis pipeline for RNA sequencing. BMC Bioinf. 15, 224.

43. Sun, Z., Evans, J., Bhagwate, A., Middha, S., Bockol, M., Yan, H., and Kocher, J.P. (2014). CAP-miRSeq: a comprehensive analysis pipeline for microRNA sequencing data. BMC Genom. 15, 423.

44. Robinson, M.D., McCarthy, D.J., and Smyth, G.K. (2010). edgeR: a Bioconductor package for differential expression analysis of digital gene expression data. Bioinformatics 26, 139–140.

45. Ru, Y., Kechris, K.J., Tabakoff, B., Hoffman, P., Radcliffe, R.A., Bowler, R., Mahaffey, S., Rossi, S., Calin, G.A., Bemis, L., and Theodorescu, D. (2014). The multiMiR R package and database: integration of microRNA-target interactions along with their disease and drug associations. Nucleic Acids Res. 42, e133.

46. Wicik, Z., Jales Neto, L.H., Guzman, L.E.F., Pavão, R., Takayama, L., Caparbo, V.F., Lopes, N.H.M., Pereira, A.C., and Pereira, R.M.R. (2021). The crosstalk between bone metabolism, lncRNAs, microRNAs and mRNAs in coronary artery calcification. Genomics 113, 503–513.

47. Wicik, Z. (2021). Wizbionet (Github).

48. Kinsella, R.J., Kahari, A., Haider, S., Zamora, J., Proctor, G., Spudich, G., Almeida-King, J., Staines, D., Derwent, P., Kerhornou, A., et al. (2011). Ensembl BioMarts: a hub for data retrieval across taxonomic space. Database 2011, bar030.

49. Guberman, J.M., Ai, J., Arnaiz, O., Baran, J., Blake, A., Baldock, R., Chelala, C., Croft, D., Cros, A., Cutts, R.J., et al. (2011). BioMart Central Portal: an open database network for the biological community. Database 2011, bar041.

50. Subramaniam, M., Pitel, K.S., Withers, S.G., Drissi, H., and Hawse, J.R. (2016). TIEG1 enhances Osterix expression and mediates its induction by TGFbeta and BMP2 in osteoblasts. Biochem. Biophys. Res. Commun. 470, 528–533.

51. Subramaniam, M., Gorny, G., Johnsen, S.A., Monroe, D.G., Evans, G.L., Fraser, D.G., Rickard, D.J., Rasmussen, K., van Deursen, J.M.A., Turner, R.T., et al. (2005). TIEG1 null mouse-derived osteoblasts are defective in mineralization and in support of osteoclast differentiation in vitro. Mol. Cell Biol. 25, 1191–1199.

52. Farr, J.N., Xu, M., Weivoda, M.M., Monroe, D.G., Fraser, D.G., Onken, J.L., Negley, B.A., Sfeir, J.G., Ogrodnik, M.B., Hachfeld, C.M., et al. (2017). Targeting cellular senescence prevents age-related bone loss in mice. Nat. Med. 23, 1072–1079.

53. Spatz, J.M., Wein, M.N., Gooi, J.H., Qu, Y., Garr, J.L., Liu, S., Barry, K.J., Uda, Y., Lai, F., Dedic, C., et al. (2015). The Wnt inhibitor sclerostin is up-regulated by mechanical unloading in osteocytes in vitro. J. Biol. Chem. 290, 16744–16758.

54. Reese, J.M., Bruinsma, E.S., Monroe, D.G., Negron, V., Suman, V.J., Ingle, J.N., Goetz, M.P., and Hawse, J.R. (2017). ERβ inhibits cyclin dependent kinases 1 and 7 in triple negative breast cancer. Oncotarget 8, 96506–96521.

55. Kaur, J., Saul, D., Doolittle, M.L., Rowsey, J.L., Vos, S.J., Farr, J.N., Khosla, S., and Monroe, D.G. (2022). Identification of a suitable endogenous control miRNA in bone aging and senescence. Gene 835, 146642.

56. Serguienko, A., Wang, M.Y., and Myklebost, O. (2018). Real-time vital mineralization detection and quantification during in vitro osteoblast differentiation. Biol. Proced. Online 20, 14.